Available online at www.sciencedirect.com
SCIENCE DIRECT
Polymer 46 (2005) 11380–11388
polymer
www.elsevier.com/locate/polymer

Linear and hyperbranched liquid crystalline polysiloxanes

Tomasz Ganicz [a,*], Tadeusz Pakula [b], Witold Fortuniak [a], Ewa Białecka-Florjańczyk [c]

[a] *Centre of Molecular and Macromolecular Studies, Polish Academy of Sciences,Sienkiewicza 112, 90-363, Łódz, Poland*
[b] *Max Planck Institute for Polymer Research, Ackermannweg 10, 55128 Mainz, Germany*
[c] *Department of General Chemistry, The High School of Agriculture, Rakowiecka 26/30, 02-653 Warsaw, Poland*

Received 10 May 2005; received in revised form 4 October 2005; accepted 4 October 2005
Available online 26 October 2005

Abstract

A series of liquid crystalline (LC) polymers having biphenyl ($-C_6H_4C_6H_4R$; R = H, $OC_{11}H_{23}$, $OC(O)CH(Cl)CH_2CH_2COOCH_2CH_3$) 4-methoxyphenyl benzoate ($-C_6H_4C(O)OC_6H_4OCH_3$) and cholesteryl type mesogenic moieties were synthesized. They were made from respective $-Si(CH_3)_2H$ terminated mesogens and vinyl functionalized linear and star shape branched polysiloxanes of comb-like and dendritic topologies and were analyzed using WAXS and SAXS techniques. Contrary to the well defined typical dendrimers, in which mesogenic groups are present in an outer sphere, the dendritic systems described here contain such groups also inside the dendritic core. It was found that star shape and dendritic LC structures exhibited various calamitic mesophases (SmA, N* and SmC*) depending on the type of mesogenic groups. On the contrary, the comb-like structures give rise to formation of hexagonal phase, even though they contain typical rod-like mesogenic moieties. For the series of 4-methoxyphenyl benzoate substituted polymers the thorough studies of the relationship between their liquid crystalline properties and topology of siloxane skeleton was determined. Mechanical properties of the LC materials were also studied.

Keywords: Liquid crystal; Hyperbranched polymer; Polysiloxane

1. Introduction

In recent years, there has been a considerable interest in polymer liquid crystals having side chain mesogenic groups. The number of reports on such structures grows exponentially since 80's due to their much improved mechanical resistance, compared to low molecular weight LC systems. However, in many applications (displays, optical data storage materials etc.) linear, high molecular weight materials exhibit too long response time in molecular order switching or rearrangement driven by changes of external electric or magnetic field. Therefore, many research groups focused their activity on hybrid or intermediate structures, especially oligomers, such as cyclic siloxanes [1] and the ones of globular shape having very distinct topologies and mechanical properties [2,3] (silsesquioxanes [4] and dendrimers [5,6]). Indeed, such studies proved that many structures of intermediate molecular weight (especially cyclic siloxanes) posses relatively high mechanical resistance and exhibit response time short enough for a number of applications [7]. However, industrial standards for opto-electronic devices are being continuously pushed forward, so there is still a lot of challenge in a search for new LC materials with precisely tunable properties, requiring deeper understanding of the property-structure relationship.

Despite already existing, extensive literature concerning LC dendrimers, dendritic or highly branched systems, which appeared over the last years, only few papers can be found, describing series of polymer LC materials with generally similar chemical structure, but different topology of their main chains [8]. Till now, mesogenic moieties have been typically incorporated into dendritic systems as fragments of main chains of the polymer skeleton [9] or as end groups located in outer sphere [10]. In many cases, it was found that the well defined dendrimers with mesogenic end groups posses a number of important physical properties, however their preparation was always a complicated and time consuming multi-step process.

Recently, we have developed a relatively easy and effective synthetic pathway, based on 'living' anionic polymerization, which lead to vinyl substituted polysiloxanes [11] of almost any type of main chain topology—linear, comb-like, star shaped and dendritic systems. Availability of such relatively well defined starting polymers having

* Corresponding author. Tel.: +48 42 6803203; fax: +48 42 6847126.
E-mail addresses: tg@bilbo.cbmm.lodz.pl (T. Ganicz), bialecka@delta.sggw.waw.pl (E. Białecka-Florjańczyk).

0032-3861/$ - see front matter © 2005 Elsevier Ltd. All rights reserved.
doi:10.1016/j.polymer.2005.10.052

different main chain topology gave us an unique opportunity to undertake in-depth studies of the effect of polymer structure on LC properties. Contrary to the previously studied dendrimeric systems, the ones described here contain functional vinyl groups not only in the outer sphere but also inside the core. Therefore, it was possible to achieve higher mass proportion of mesogenic moieties in a macromolecule, with respect to the main polymer skeleton.

2. Experimental

2.1. Materials and characterization methods

All the reactions were carried out under argon with exclusion of moisture. Solvents—Et_2O, THF, toluene were dried by standard methods and stored over sodium mirror or molecular sieves. CH_2Cl_2, methanol, pentane, cholesterol (Fluka), MeLi (1.3 M solution in Et_2O) (Aldrich), $LiAlH_4$ (Fluka), chlorodimethylsilane ($HSiMe_2Cl$) (ABCR) and 1,1,3,3-tetramethyldisiloxane (Aldrich) were used as received.

Syntheses of starting vinyl substituted polysiloxanes, as well as the methods of evaluating their structure and molecular weight have been already described [11]. Karstedt's catalyst ($Pt_2[(ViMe_2Si)_2O]_3$, 3–3.5% of Pt in xylenes) (ABCR) have been used as supplied.

4-(Pent-4-enyloxy)biphenyl [CH_2=$CH(CH_2)_3OC_6H_4C_6H_5$], 4-(pent-4-enyloxy)-benzoic acid 4-methoxyphenyl ester [CH_2=$CH(CH_2)_3OC_6H_4C(O)OC_6H_4OCH_3$], 4-undecyloxy-4′-(pent-4-enyloxy)biphenyl [CH_2=$CH(CH_2)_3OC_6H_4C_6H_4OC_{11}H_{23}$] (S)-2-chloropentanedioic acid 5-ethyl ester 1-(4′-undec-10-enyloxybiphenyl-4-yl) ester [CH_2=$CH(CH_2)_9OC_6H_4C_6H_4O(O)CCH(Cl)CH_2CH_2C(O)OC_2H_5$] were made according to literature methods [12–14].

^1H and ^{13}C NMR spectra were recorded using Brucker DRX 200 and 500 MHz machines. FTIR spectra were obtained with ATI Mattson spectrometer.

2.2. Mesogenes with Si–H terminal groups

The synthesis of mesogenes with terminal Si–H groups has been performed in three different ways. [5-(biphenyl-4-yloxy)-pentyl]-dimethylsilane [$HSiMe_2(CH_2)_5OC_6H_4C_6H_5$] (**1**) and [5-(4′-undecyloxybiphenyl-4-yloxy)-pentyl]-dimethylsilane [$HSiMe_2(CH_2)_5OC_6H_4C_6H_4OC_{11}H_{23}$] (**2**) were obtained by reaction of $H(Me)_2SiCl$ with appropriate terminal alkenes and subsequent reduction of Si–Cl bonds to Si–H ones using $LiAlH_4$ [15]. 4-[(5-dimethylsilanyl)pentyloxy]-benzoic acid 4-methoxyphenyl ester [$HSiMe_2(CH_2)_3OC_6H_4C(O)OC_6H_4OCH_3$] (**3**) and (S)-2-chloropentanedioic acid 5-ethyl ester 1-{4′-[11-(1,1,3,3-tetramthyldisiloxanyl)-undecyloxy]-biphenyl-4-yl} ester [$HSiMe_2OSiMe_2(CH_2)_{11}OC_6H_4C_6H_4O(O)CCH(Cl)CH_2CH_2C(O)OC_2H_5$] (**4**) were made by hydrosilylation of the respective terminal alkenes with large excess (1000%) of tetramethyldisiloxane ($HSiMe_2OSiMe_2H$) [15].

Synthesis of cholesteryloxydimethylsilane (**5**) was carried out as follows. MeLi (9.24 ml, 12.94 mmol) of 1.4 M sol. in Et_2O was added dropwise to a solution of cholesterol (5 g, 12.93 mmol) in THF (20 ml) during 15 min at room temperature (~22 °C). The mixture was stirred for further 3 h at room temperature, under argon, yielding yellow solution of lithiated cholesterol. $HSi(Cl)Me_2$ (1.4 ml, 12.93 mmol) was added dropwise to the solution within 15 min. at room temperature. The mixture was stirred for further 12 h. Solvents were evaporated under vacuum, and the white residue was extracted with dry pentane and filtered under argon. The pentane was evaporated under vacuum leaving white, crystalline cholesteryloxydimethylsilane, which was purified by crystallization from dry methylcyclohexane. Yield: 4.73 g (82%) ^1H NMR: ($CDCl_3$) δ: 0.28 (6H, s, SiMe), 0.89–2.28, [C(sp^3)-H resonances in cholesteryl group], 4.67 (1H, m, Si–H), 5.36 (2H, d, HC=CH in cholesteryl group). ^{29}Si NMR (INEPT—$CDCl_3$): −6.3.

2.3. Reverse hydrosilylation of vinyl substituted polysiloxanes with $Si(Me)_2H$ terminated mesogenes

All hydrosilylations leading to polysiloxanes with mesogenic substituents at silicon atoms, independently of their topology and molecular weight, were performed according to the general procedure described below:

A solution of poly(methylvinylsiloxane) (7 mmol of vinyl groups) and Si–H terminated mesogen (7.7 mmol of Si–H) in dry toluene (10 ml) was stirred in a flamed Schlenk tube under argon and Karstedt's catalyst (20 μl, 5.1×10^{-4} mol Pt/mol Vi) was added. The reaction mixture was stirred at 60 °C (time is given in Table 1). Progress of reaction was followed by FTIR (disappearance of Si–H absorption at ~2110–2180 cm^{-1}). Solvent was removed under vacuum, and polymer was purified by several precipitations from CH_2Cl_2/MeOH mixtures, centrifuged and finally dried under vacuum (1 mmHg, 80–90 °C). Basic characteristics of polymers (GPC, topology and structures of mesogenic side chains and yields) are given in Table 1.

NMR data:

B-I-1: ^1H NMR (C_6D_6) δ: 0.07–0.24, (m, $SiMe_2$), 0.45–0.68 (m, Si–CH_2), 1.75–1.82 (m, Si–CH_2CH_2), 3.79 (t, OCH_2), 6.93–7.65 (m, aromatic protons). ^{29}Si NMR (C_6D_6, INEPT): −21.2 ($OSiMe_2$), −12.6 (OSiMeR), −3.1 ($OSiMe_3$—end groups), 2.6 (C–Si–C in side mesogenic chains).

B-II-1: ^1H NMR (C_6D_6) δ: 0.11–0.25 (m, SiMe), 0.55–0.62 (m, Si–CH_2), 1.73–1.84 (m, Si–CH_2CH_2), 3.75 (t, OCH_2), 5.90–6.20 (m, traces of unreacted Si–Vi), 6.95–7.65 (m, aromatic protons). ^{29}Si NMR (C_6D_6, INEPT): −19.8 to −17.2 (OSiMe and $OSiMe_2$), 2.7 (C–Si–C in side mesogenic chains).

D-II-1: ^1H NMR (C_6D_6) δ: 0.12–0.25, (m, $SiMe_2$), 0.53–0.60 (m, Si–CH_2), 1.70–.82 (m, Si–CH_2CH_2), 3.79 (t, OCH_2), 5.90–6.05 (m, traces of unreacted Si–Vi), 6.95–7.65 (m, aromatic protons). ^{29}Si NMR (C_6D_6, INEPT): −22.8 to −12.6 (OSiMeR and $OSiMe_2$), 2.5 (C–Si–C in side mesogenic chains).

B-II-2: ^1H NMR (C_6D_6) δ: 0.15–0.25, (s, $SiMe_2$), 0.28 (s, CH_3–C), 0.53–0.65 (m, Si–CH_2), 1.15–1.55 (m, C–CH_2–C), 1.68–1.73 (m, OCH_2CH_2), 3.75 (t, OCH_2), 6.95–7.26 (m, aromatic protons). ^{29}Si NMR (C_6D_6, INEPT): −18.6 to

Table 1
'Reverse' hydrosilylation reaction conditions and transition temperatures of resulting LC polymers

Sample/Polymer type	Mesogen	Starting polymer		Products	
		M_n (^{1}H NMR)	Number and M_n of last gen.-arms.	'Vinyl group density'	Conversion/ reaction time	Phase transtion
B-I-1 Linear	1	3600	1−M_n=3600	11.1 mmol Vi/g	>95%/48 h	K 43 N[a] 62 I
B-II-1 Brush (II-gen.)	1	33,400	Around 13 of M_n=1200	8.75 mmol Vi/g	75%/48 h	None
D-II-1 Dendrimer on star (II-gen)	1	69,000	Around 6 of M_n=1200	4.3 mmol Vi/g	82%/72 h	None
B-II-2 Brush (II-gen)	2	33,400	Around 13 of M_n=1200	8.75 mmol Vi/g	>95%/96 h	K 57 N[a] 89 I
B-I-3 Brush I (linear)	3	3600	1−M_n=3600	11.1 mmol Vi/g	100%/96 h	T_g−16 SmA[a] 78 I
B-II-3 Brush (II gen.)	3	34,300	Around 13 of M_n=1300	8.75 mmol Vi/g	100%/96 h	T_g-19 SmA[a] 58 I
D-II-3 Dendrimer on 'brush' (II-gen)	3	760,000	Around 550 of M_n=1400	8.6 mmol Vi/g	100%/96 h	T_g−18 SmA[a] 69 I
D-I-3 'Star' (Dendrimer (I gen))	3	6200	4−M_n=1500	11 mmol Vi/g	100%/96 h	T_g-15 SmA[a] 77 I
D-III-3 Dendrimer on 'brush' (III-gen)	3	1,350,000	Around 1000 of M_n=550	8.5 mmol Vi/g	65%/96 h	None
B-I-4 Brush I (Linear)	4	3 600	1−M_n=3600	11.1 mmol Vi/g	61%/96 h	K 75 SmC*[b] 106 I
D-I-4 'Star' (Dendrimer I-gen)	4	6200	4−M_n=1500	11 mmol Vi/g	46%/96 h	T_g−17 SmC*[b] 96 I
B-I-5 Brush I (linear)	5	8700	1 of M_n=8700	5.7 mmol Vi/g	57%/96 h	K 68 N*[b] 79 I
B-II-5 Brush (II gen.)	5	33,400	Around 13 of M_n=1200	8.75 mmol Vi/g	46%/96 h	T_g-16 N*[b] 64 I
D-II-5 Dendrimer on star (II-gen)	5	69,000	Around 6 of M_n=1200	4.3 mmol Vi/g	53%/96 h	None

T_g , glassy state; N, nematic; N*, cholesteric; SmA, smectic A; SmC*, chiral smectic C; M_n, number average molecular weight; Vi/g, molar amount of vinyl groups per 1 g of polymer; h, hours.
[a] WAXS and polarizing optical microscopy.
[b] Polarizing microsocopy only.

−12.4 (OSiMeR and $OSiMe_2$), 2.2 (C–Si–C in side mesogenic chains).

B-I-3: ^{1}H NMR (C_6D_6) δ:, 0.05–0.20 (s, $SiMe_2$), 0.45–0.55 (m, Si–CH_2), 1.10–1.14 (m, Si–CH_2CH_2), 1.40–1.60 (m, $SiCH_2CH_2CH_2$), 1.72–1.75 (m, CH_2CH_2O), 3.76 (s, OCH_3), 3.95–4.05 (m, OCH_2), 6.95, 7.12, 8.05 (m, aromatic protons). ^{29}Si NMR (C_6D_6, INEPT): −22.4 to −20.9 (OSiMe -in main chain), −18.3 to −17.4 ($OSiMe_2CH_2$ from disiloxane moieties in side mesogenic chains).

B-II-3: ^{1}H NMR (C_6D_6) δ:, 0.02–0.18 (s, $SiMe_2$), 0.40–0.58 (m, Si–CH_2), 1.15–1.60 (m, C–CH_2–C), 1.73–1.82 (m, CH_2CH_2O), 3.75 (s, OCH_3), 4.03 (t, OCH_2), 6.95–8.05 (m, aromatic protons). ^{29}Si NMR (C_6D_6, INEPT): −21.3 to −19.1 (OSiMe—in main chain), −18.1 to −17.2 ($OSiMe_2CH_2$ from disiloxane moieties in side mesogenic chains).

D-II-3: ^{1}H NMR (C_6D_6) δ: −0.05–0.27 (m, $SiMe_2$), 0.32–0.56 (m, Si–CH_2), 1.12–1.65 (m, C–CH_2–C), 1.75–1.80 (m, CH_2CH_2O), 3.77 (s, OCH_3), 4.01 (t, OCH_2), 6.95–8.05 (m, aromatic protons). ^{29}Si NMR (C_6D_6, INEPT): −21.6 to −19.1 (OSiMe—in main chain), −18.9 to −17.4 ($OSiMe_2CH_2$ from disiloxane moieties in side mesogenic chains).

D-I-3: ^{1}H NMR (C_6D_6) δ:0.08–0.19 (s, $SiMe_2$), 0.48–0.55 (m, Si–CH_2), 1.10–1.14 (m, Si–CH_2CH_2), 1.45–1.55 (m, $SiCH_2CH_2CH_2$), 1.72–1.81 (m, CH_2CH_2O), 3.77 (s, OCH_3), 3.95 (t, OCH_2), 6.95–8.05 (m, aromatic protons). ^{29}Si NMR (C_6D_6, INEPT): −23.4 to −19.8 (OSiMe—in main chain), −18.7 to −17.9 ($OSiMe_2CH_2$ from disiloxane moieties in side mesogenic chains).

D-III-3: ^{1}H NMR (C_6D_6) δ: 0.08–0.30 (m, SiMe), 0.35–0.49 (m, Si–CH_2), 1.18–1.55 (m, C–CH_2–C), 1.73–1.82 (m, CH_2CH_2O), 3.75 (s, OCH_3), 4.01 (t, OCH_2), 5.92–6.25 (m, traces of unreacted Si–Vi), 6.94–8.06 (m, aromatic protons). ^{29}Si NMR (C_6D_6, INEPT): −22.3 to −19.4 (OSiMe—in main chain), −18.2 to −17.8 ($OSiMe_2CH_2$ from disiloxane moieties in side mesogenic chains).

B-I-4: ^{1}H NMR (C_6D_6) δ: 0.05–0.25 (m, $SiMe_2$), 0.45–0.55 (m, Si–CH_2), 1.25–1.50 (m, CH_2–CH_2–CH_2+CH(Cl)CH_3), 1.78–1.85 (m, CH_2CH_2O), 3.95–4.23 (m, OCH_2), 2.51–2.63

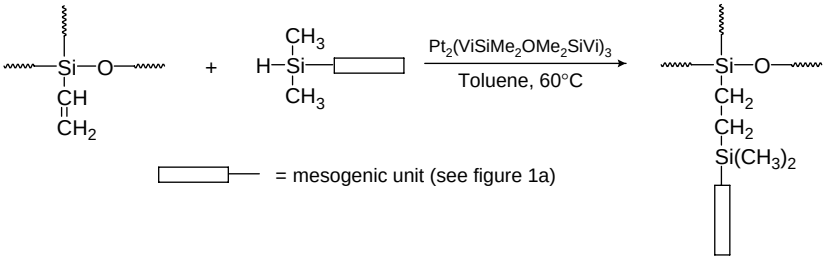

Scheme 1. 'Reverse' hydrosilylation process, leading to LC polymers.

(m, CH_2CO), 5.76–6.10 (m, traces of unreacted Si–Vi), 6.42–6.45 (m, CHCl), 6.85–7.83 (m, aromatic protons), ^{29}Si NMR (C_6D_6, INEPT): −21.3 to −20.8 (OSiMe—from main chain), −18.6 to −17.2 ($OSiMe_2CH_2$ from disiloxane moieties in side mesogenic chains).

D-I-4: ^{1}H NMR (C_6D_6) δ: 0.07–0.28 (m, $SiMe_2$), 0.43–0.56 (m, Si–CH_2), 1.23–1.64 (m, CH_2–*CH_2*–CH_2 + CH(Cl)*CH_3*), 1.75–1.86 (m, *CH_2*CH_2O), 3.93–4.30 (m, OCH_2), 2.50–2.65 (m, CH_2CO), 5.92–6.26 (m, traces of unreacted Si–Vi), 6.43–6.46 (m, CHCl), 6.83–7.85 (m, aromatic protons), ^{29}Si NMR (C_6D_6, INEPT): −22.6 to −19.1 (OSiMe—in main chain), −18.6 to −17.3 ($OSiMe_2CH_2$ from disiloxane moieties in side mesogenic chains).

B-I-5: ^{1}H NMR (C_6D_6) δ: 0.05–0.26, (s, $SiMe_2$), 0.43–0.52 (m, Si–CH_2), 0.85–2.1 (m, C-sp^3-H from cholesterol + C–CH_2C–C), 2.21–2.24 (m, *CH_2*CH_2O), 3.27 (t, CH_2O), 5.28–5.32 (m, –HC=CH– from cholesterol), 5.75–6.23 (m, traces of unreacted Si–Vi). ^{29}Si NMR (C_6D_6, INEPT): −22.3 ($OSiMe_2$), −12.8 (OSiMeR), −3.02 ($OSiMe_3$ end groups), 2.8 (C–Si–C from side mesogenic chains).

B-II-5: ^{1}H NMR (C_6D_6) δ: 0.06–0.23, (m, $SiMe_2$), 0.42–0.56 (m, Si–CH_2), 0.86–2.15 (m, C-sp^3-H from cholesterol + C–CH_2C–C), 2.25–2.31 (m, *CH_2*CH_2O), 3.26 (t, CH_2O), 5.30–5.34 (m, –HC=CH– from cholesterol), 5.73–6.31 (m, traces of unreacted Si–Vi). ^{29}Si NMR (C_6D_6, INEPT): −21.8 to −19.4 (OSiMe—in main chain), 2.3 (C–Si–C from side mesogenic chains).

D-II-5: ^{1}H NMR (C_6D_6) δ: 0.03–0.28, (m, $SiMe_2$), 0.44–0.59 (m, Si–CH_2), 0.85–2.14 (m, C-sp^3-H from cholesterol + C–CH_2C–C), 2.24–2.29 (m, *CH_2*CH_2O), 3.27 (t, CH_2O), 5.32–5.36 (m, –HC=CH– from cholesterol), 5.70–6.41 (m, traces of unreacted Si–Vi). ^{29}Si NMR (C_6D_6, INEPT): −21.9 to −19.2 (OSiMe—in main chain), +2.2 (C–Si–C from side mesogenic chains).

2.4. Structural characterization and properties in bulk

Thermal properties were studied with differential scanning calorimetry (DSC) using a DuPont DSC-910, calibrated with an indium standard. Phase transitions were verified by optical microscopy.

Wide angle X-ray Scattering (WAXS) techniques have been used to characterize the structure. Measurements have been performed at room temperature using a θ–θ diffractometer (Siemens), as well as a 2D position sensitive detector with a pin-hole collimation of the incident beam. Cu K_α radiation ($\lambda = 0.154$ nm) was used. The recorded scattered intensity distributions are presented as functions of the scattering vector ($s = 2 \sin\theta/\lambda$, where 2θ is the scattering angle). The 2D scattering patterns have been recorded for filaments macroscopically oriented by extrusion in the temperature range ~10–20 K below the isotropization temperature, using a mini-extruder described elsewhere [16].

Mechanical characterization has been performed using the ARES mechanical spectrometer (Rheometric Scientific). Shear deformation has been applied under conditions of controlled deformation amplitude which was changed with temperature between $\Delta\gamma = 0.0001$ at low temperatures and $\Delta\gamma = 0.05$ at high temperatures, but always remaining in the range of the linear viscoelastic response of studied samples. Plate-plate geometry has been used with plate diameters of 6 mm. The samples were placed between plates and pressed at room temperature to obtain the gap between plates (sample thickness) of about 1 mm. Experiments have been performed under dry nitrogen atmosphere. Temperature dependencies of

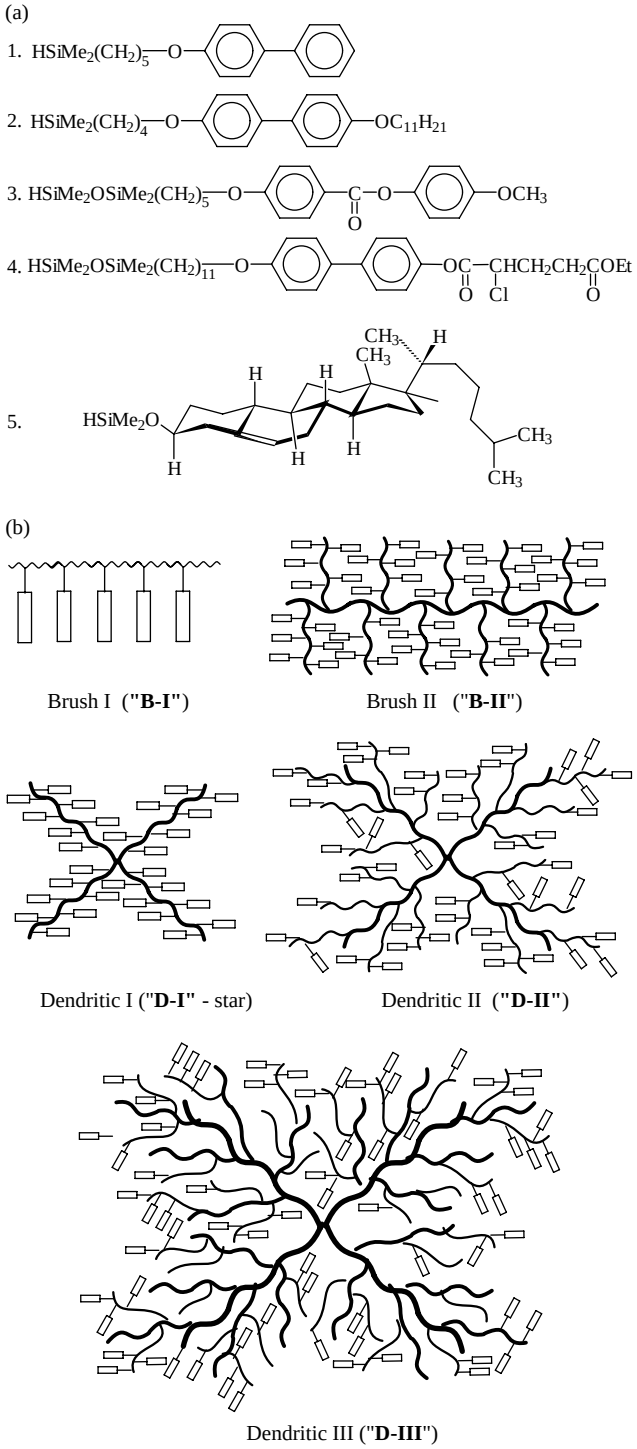

Fig. 1. Structures of starting Si–H containing mesogenes (a) and mesogen substituted polymers (b).

Table 2
Transition temperatures, microstructures, X-ray Bragg spacings (d) and dynamic viscosities (η^*) of selected polymers

Sample	Mesogen	T_g (°C)	T_i (°C)	d (nm) structure	η^*(Pa s)
B-II-2 Brush (II-gen)	2			3.6 undefined	–
B-I-3 Brush I (linear)	3	−16	78	2.95 lamellar	6.7
B-II-3 Brush (II gen.)	3	−19	58	3.3 square	47
D-I-3 'Star' (Dendrimer (I gen))	3	−15	77	2.91 lamellar	15.5
D-II-3 Dendrimer on 'brush' (II-gen)	3	−18	69	3.0 lamellar	1294

d, Bragg spacing corresponding to the maximum of the broad small-angle peak characteristic of the phase; η^*, dynamic viscosity.

the real, G', and imaginary, G'', parts of the complex shear modulus were determined at a constant deformation frequency of 10 rad/s. under continuous cooling of samples with the rate of 2 °C/min. The dependencies are used to characterize the properties within the broad temperature range extending between −100 and 180 °C.

3. Results and discussion

3.1. Synthetic pathways

LC side chain polysiloxanes are typically synthesised by hydrosilylation of mesogenic terminal alkenes with polymers having reactive Si–H moieties. However, the synthesis of Si–H containing branched system is complicated, whereas the synthetic route, leading to polysiloxanes, bearing vinyl moieties, having wide range of possible topologies of their main chains have been recently developed in our laboratory [11]. Therefore, we tried the other approach, leading to LC polysiloxanes via so called 'reverse hydrosilylation' (Scheme 1).

The reaction was carried out under conditions similar to those used in typical hydrosilylations of mesogenic alkenes [7], except for the use of 10% excess of Si–H terminated mesogens, reverse to the normally used excess of terminal alkenyl or vinyl moieties. The main purpose of using excess of Si–H terminated mesogenic compounds was to achieve as high addition to vinyl groups as possible. According to theoretical considerations derived from general mechanism of hydrosilylation process, [17] the excess of vinyl groups is necessary for the formation of an active Pt–Vi complexes. Contrary to this view, reactions with excess of Si–H moieties underwent smoothly and it was usually completed within 24–72 h. However, in the case of dendritic polymers of higher generations, it was impossible to obtain complete addition to all vinyl groups even after prolonged reaction time (See e.g. D-III-3 in Table 1: 96 h; 65% addition). We believe, though that long reaction time and incomplete addition was mainly due to increased steric hindrance of branched systems and not the relatively low Vi/SiH molar ratio. It must be stressed that dendritic polymers synthesized here contained vinyl moieties not only in the outer sphere, and for higher generations the access to the inner ones, by relatively large mesogenic compounds with terminal Si–H groups, became increasingly difficult.

Certain complication of the 'reverse' hydrosilylation approach was a preliminary modification of mesogenes in such a way that they contained terminal Si–H moieties. We have developed three different methods leading to such compounds. The first one involved hydrosilylation of a mesogen terminal alkenyl group with $HSiMe_2Cl$ and subsequent reduction of Si–Cl to Si–H moiety. The method was simple and effective but limited to mesogenic systems, which did not contain ester, cyano and other organic groups prone to $LiAlH_4$. Thus, it could be applied only to the mesogenic compounds of biphenyl type (structures 1 and 2 in Fig. 1(a)).

The second method was also based on hydrosilylation of mesogenes bearing terminal alkene groups, but the source of Si–H moieties was tetramethyldisiloxane ($HSiMe_2OSiMe_2H$). In this case there is no limitation for the structure of a mesogen, as the reduction step ($LiAlH_4$) was avoided, but the process required large excess (more than 100%) of disiloxane in order to avoid double substituted side product ($RSiMe_2OSiMe_2R$) instead of the desired ($HSiMe_2OSiMe_2R$). However, even with large excess of disiloxane small amount of side product was

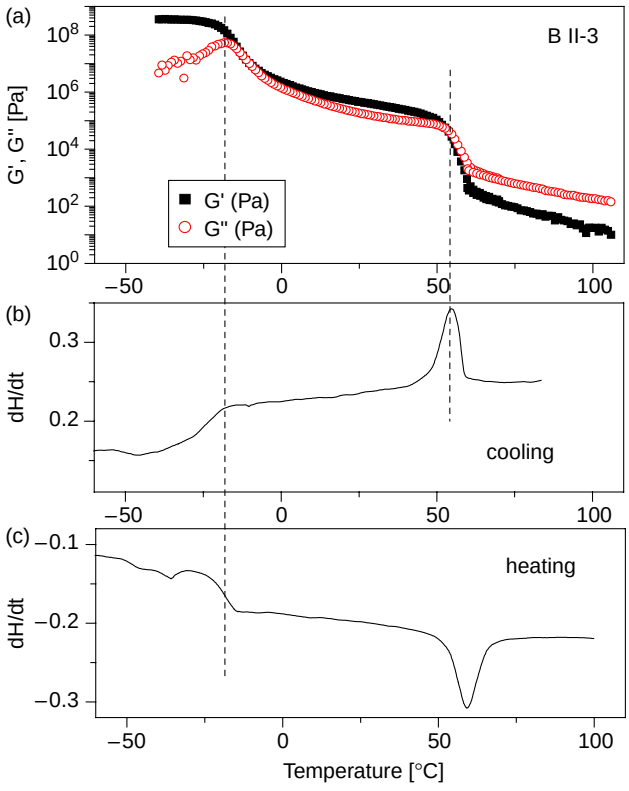

Fig. 2. Dynamic mechanical (a) and DSC ((b) and (c)) data for B-II-3 sample (brush-like, second generation with 4-methoxyphenyl benzoate mesogenes). Mechanical analyses were performed on cooling at the rate of 2 °C/min. The DSC measurements, both for cooling (b) and heating (c) runs, were performed at the rate of 10 °C/min.

always formed, though it could be easily removed from a final polymer by subsequent precipitation from CH_2Cl_2/MeOH. (structures 3 and 4 in Fig. 1(a)).

The third method was used for cholesteryl derivative only. The dimethylsilyl modified cholesterol was obtained in a simple, one step reaction of lithium cholesterate with dimethylchlorosilane (HMe_2SiCl), at low temperature. The method can be applied only to the systems with terminal hydroxy function, which do not contain any other groups prone to reaction with MeLi (structure 5 in Fig. 1(a)).

3.2. Structure–properties relationship

As it can be seen (Table 1) not all the polymers exhibit good LC properties. Some of them do not generate mesophases, probably due to low 'density' of mesogenic groups (for example: D-II-1) along their main chains, while in other cases, probably due to the weak mesogenic properties of simple biphenyl rod-like structures (D-I-1). The 'density' of mesogenic groups varied not only because of the amount of vinyl groups in starting polymers, but also due to problems with achieving 100% completion of hydrosilylation reaction. Polymers with high enough 'density' (at least 5 mol/g) of stronger mesogenic moieties generate various mesophases (nematic, smectic and columnar) in a quite wide range of temperature. For all the polymers exhibiting LC properties (except D-II-3) the type of mesophase depends on the structure of mesogenic moieties only, no matter what the topology of their main chains. We believe, that small differences of the 'density' of mesogenic groups resulting form incomplete hydrosilylation did not affect LC properties significantly, pointed that more than 80% of vinyl groups underwent addition. The LC properties of D-II-3 sample will be discussed below, separately.

For detailed structure-properties relationship studies we have chosen the series of polymers having 4-methoxyphenyl benzoate mesogenic moieties obtained from hydrosilylation with compound **3**. This structure was often used for such studies in the past [18]. Within this series the conversion of vinyl groups was in the range of 96–100%. Results were compared with polymer B-II-2 bearing undecenyloxybiphenyl groups, obtained from compound **2**. The respective phase transition temperatures and structural properties are summarized in Table 2.

A typical thermo-mechanical behavior of the studied materials is shown in Fig. 2. Temperature dependency of the real (G') and imaginary (G'') components of the complex shear

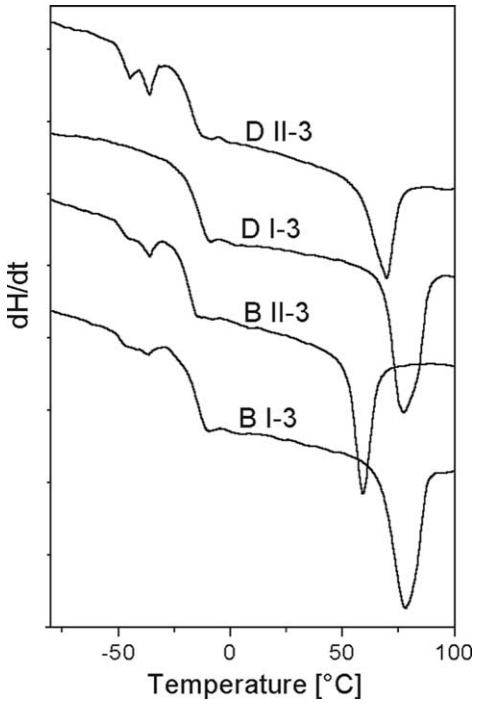

Fig. 3. DSC traces from the second heating run for the four samples with different molecular architecture, having the same mesogen unit (no. 3,4-methoxyphenyl benzoate).

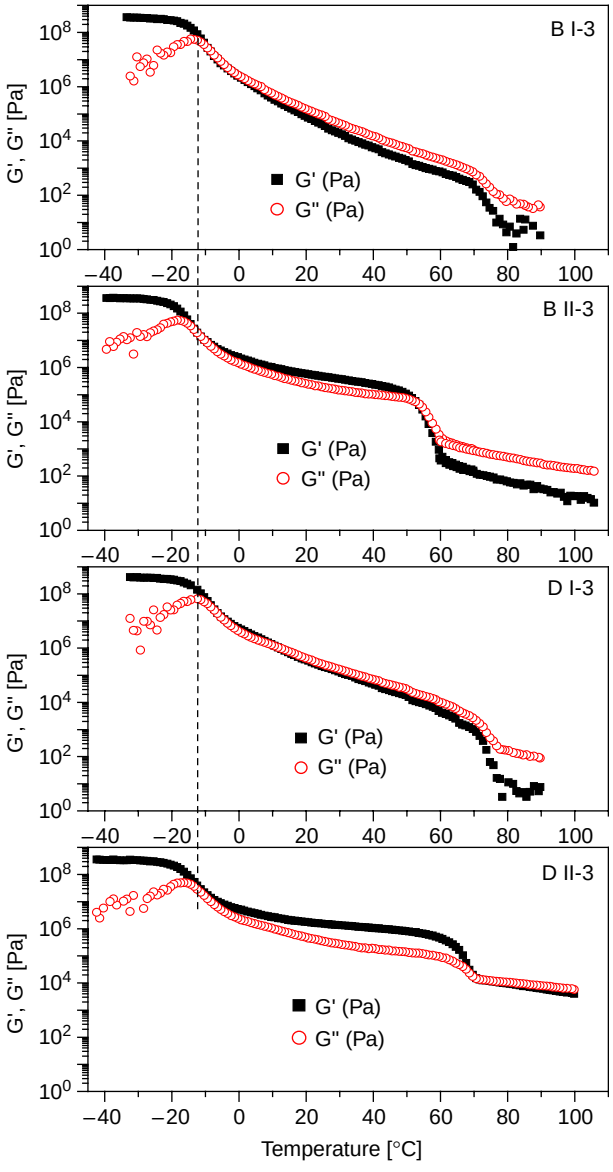

Fig. 4. Dynamic mechanical results (real, G', and imaginary, G''parts of the complex vs temperature, T) for the four samples with different molecular architecture, having the same mesogen unit (no. 3,4-methoxyphenyl benzoate).

modulus (Fig. 2(a)) recorded on cooling from the molten isotropic state are compared with DSC thermograms (Fig. 2(b) and (c)) run for both cooling and heating. The mechanical and calorimetric measurements performed under cooling indicate characteristic transitions which can be attributed to formation of a mesophase close to 60 °C and transition to a glassy state at ~ −20 °C.

Accordingly, the mechanical data indicate material flow at high temperatures, a rubber-like behavior in the mesophase (with modulus in the range of 10^5 Pa) and the glassy state with modulus $G' > 10^8$ Pa. On heating (Fig. 3(c)), the transitions take place at slightly higher temperatures than under cooling.

A comparison of the DSC thermograms for samples of various architectures, recorded under heating, is shown in Fig. 3. Transition temperatures determined from these results are given in Table 2. They show that the glass transitions in these systems are nearly the same but the isotropization temperature seems to correlate with the molecular architecture or related composition variation in the samples. For systems of the first generation, both comb-like and dendritic polymers, for which vinyl group density is of 11 mmol/g, transition temperatures are by more than 10 °C higher compared to these for the corresponding systems of second generation having vinyl group density slightly below 9 mmol/g. Probably, a composition related effect is also observed below the glass transition where melting of the spacer phase seems to take place with higher intensity, the lower density of vinyl groups.

In Fig. 4, mechanical properties of the systems having various molecular architectures but the same mesogen (structure 3) are compared. In all cases, the three phases mentioned above, i.e. glassy, mesophase and isotropic melt are well distinguishable and the transitions between them coincide well with those determined by DSC (Fig. 3). Properties of glassy states are nearly identical for these samples, while differences arise in the other phases. The samples of the first generation—brush-type or dendritic macromolecules exhibit a gel-like behavior in the mesophase with properties continuously varying with temperature. In isotropic melts all of them show a rather low viscosity. On the other hand, macromolecules of corresponding second generations become rubber-like in the mesophase, with G' plateau stable over a broad temperature range and flow in the melt but with considerably higher viscosities than for the corresponding first generation

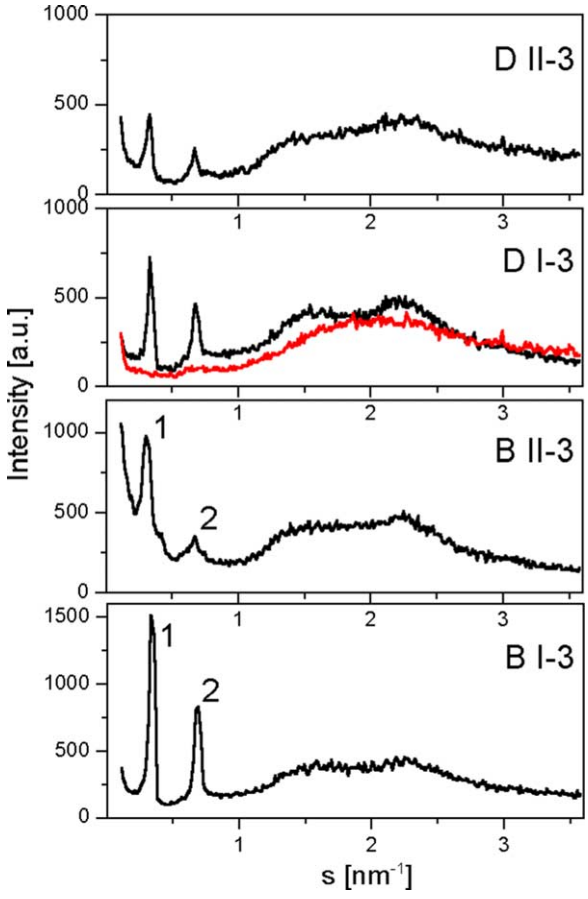

Fig. 5. Wide angle X-ray diffractograms recorded at room temperature for the four samples with different molecular architecture, having the same mesogen unit (no. 3,4-methoxyphenyl benzoate). Additionally, intensity distribution recorded above isotropisation temperature is shown for star-shape system (D-I-3).

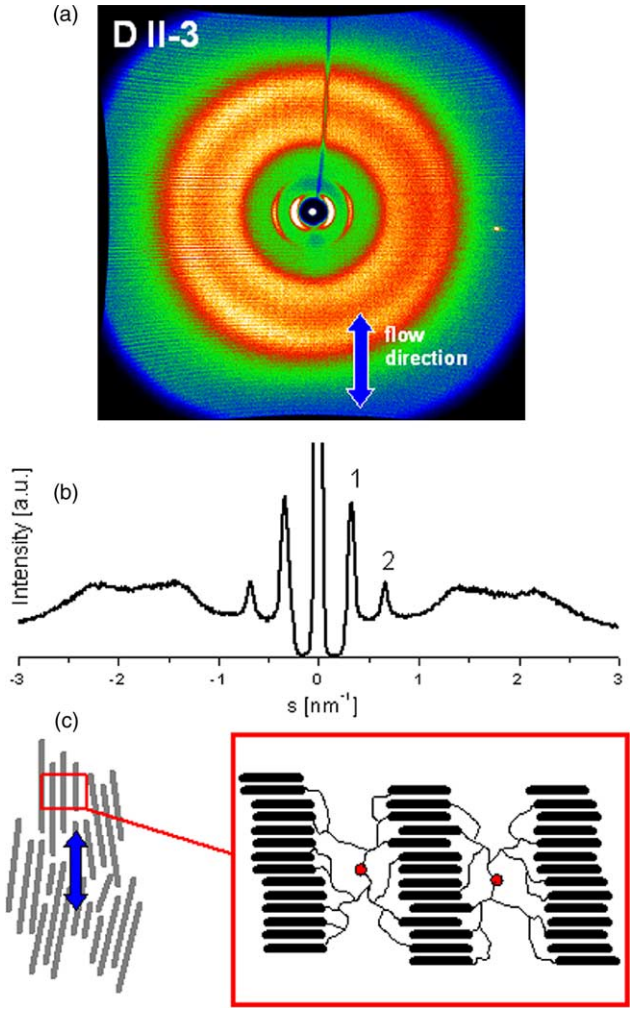

Fig. 6. (a) Two-dimensional X-ray diffraction pattern recorded for oriented filament of dendrimer-type polysiloxane with 4-methoxyphenyl benzoate mesogenic moieties (D-II-3); (b) equatorial intensity distribution pattern; (c) schematic morphology of the material.

macromolecules. The latter effect can be attributed to the differences in sizes of the macromolecules. Individual viscosity values for the four samples are given in Table 2.

Details concerning mesophase structures were obtained from X-ray diffraction studies and the results are summarized in Fig. 5. In most cases, they indicate a layer-like correlation with the characteristic first and second order Bragg intensity maxima being in relative positions 1 and 2. The correlation period detected, varies only slightly for the samples, most probably as a result of similar mesogen densities. Mesophase ordering for second generation brush-like system (B-II-3) appears to be slightly different. The positions of intensity maxima suggest a square lattice which can only be attributed to laterally arranged, elongated structural units i.e. columns.

The mesophase structures can be characterized more precisely, when the X-ray scattering is recorded for macroscopically oriented samples. Such samples have been prepared by cold extrusion at room temperature, which for all samples analyzed here is nearly half way through the mesophase temperature range. Two examples are shown in Figs. 6 and 7. Fig. 6 shows the pattern obtained for a dendritic polymer of second generation (D-II-3) which can be considered also as a typical one for the first generation macromolecules. The 2D diffraction pattern indicates an amorphous, almost isotropic halo at wide angles and intensive equatorial reflections at low scattering angles, confirming thus the intensity distributions presented in the Fig. 5. At the bottom of the Fig. 6, the suggested morphology is illustrated schematically. A quite considerable azimuthal width of the low angle, near equatorial reflections, indicate non perfect morphological orientation of the structural elements. Therefore, a structure consisting of grains of locally better correlated layers is postulated.

Analogous documentation of the pattern for the B-II-3 comb-like polymer is presented in Fig. 7. The equatorial intensity distribution confirms, in this case, a different lateral order, of structure aligned better than in the former case. Columnar morphology is postulated with columns aligned along the deformation direction and creating local square lattices.

It is interesting that for well defined dendritic systems, having mesogenic moieties in the outer sphere, only a similar columnar phase was observed for higher generation (4 or 5) globular systems, while polymers with lower generation (2 or 3) generate a rather typical calamitic mesophase (smectic or even nematic) [12,19].

The type of mesogen can have significant effect on the structure and properties of the system, into which it is

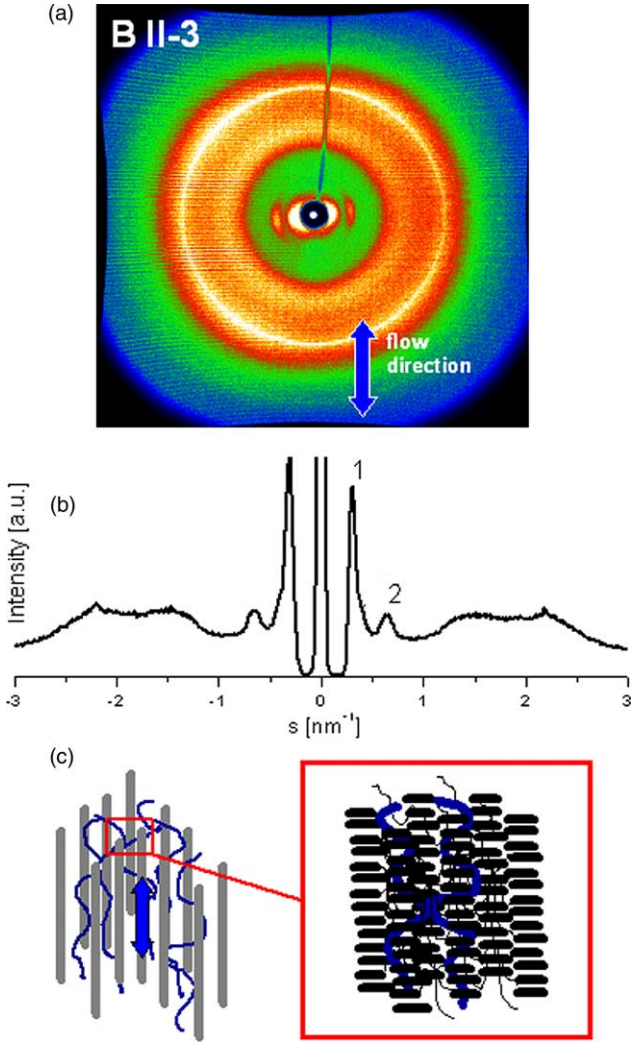

Fig. 7. (a) Two-dimensional X-ray diffraction pattern recorded for oriented filament of the brush-type polysiloxane with 4-methoxyphenyl benzoate mesogenic moieties (B-II-3); (b) equatorial intensity distribution pattern; (c) schematic morphology of the material.

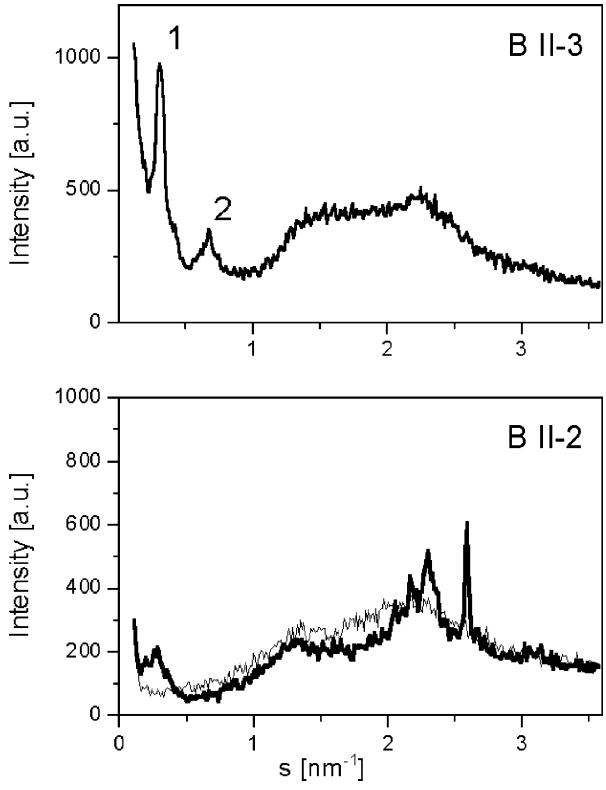

Fig. 8. Effect of mesogen type on the structure as observed by WAXS. In the bottom figure, intensity distributions recorded at 27 °C—thick line (mesophase) and 100 °C—thin line (melt).

incorporated. An example is shown in Fig. 8 where it can be seen that the alteration of the mesogen within the same chain architecture can drastically change the diffraction pattern and consequently local and long range ordering of the system.

4. Conclusions

The synthetic pathway based on 'reverse hydrosilylation' proved to be effective for preparation of LC polysiloxanes with a wide range of topologies of their main chains. The set of polymers with same type of mesogenic moieties but different structure of their main chains gave a unique opportunity to study LC properties—structure relationship. It was found that dendritic type topology of polymers leads to shorter temperature range of mesophase formation and lower molecular order in comparison with analogous brush-like systems. A second generation brush-type topology is much more advantageous in terms of strong LC properties of the resulting materials. It was also found that brush-type structures have a tendency to form columnar phases instead of the calamitic ones, even if they incorporate typical rod-like mesogenic units. The dendritic liquid crystal systems, presented here require the density of mesogenic units in the range of 9–11 mmol/g which means that they should be present also in the inner core of the macromolecule. It points to the importance of deep interpenetration and interaction of individual mesogens originating from various spherical macromolecules.

References

[1] Richards RDC, Hawthorne WD, Hill JS, White MS, Lacey D, Semlyen JS, et al. J Chem Soc, Chem Commun 1991;95:104–15.
[2] Obrecht W, Seitz U, Funke W. Macromol Chem 1978;179: 2145–52.
[3] Stutz H. J Polym Sci, Part B: Polym Phys 1995;33:333–8.
[4] Saez IM, Styring P. Adv Mater 1996;8:1001–5.
[5] Friberg ES, Podzimek M, Tomalia DA. Mol Cryst Liq Cryst 1988;164: 157–68.
[6] Elsasser R, Goodby JW, Mehl GH, Rodrigues-Martin D, Richardson RM, Photions DJ, et al. Mol Cryst Liq Cryst 2003;402:237–43.
[7] Bunning TJ, Kreuzer FH. Trends Polym Sci 1995;3:318–26.
[8] Mehl GH, Thornton AJ, Goodby JW. Mol Cryst Liq Cryst 1999;332: 2965–71.
[9] Bauer S, Fisher H, Ringsdorf H. Angew Chem Int Ed Engl 1993;32: 1589–993. Percec V, Chu P, Kawasumi M. Macromolecules 1994;27: 4441–53.
[10] Barbera J, Donnio B, Gimenez R, Guillon D, Marcos M, Omenat A, et al. Macromolecules 2002;35:370–82. Zhu X-M, Boiko NI, Rebrov EA, Muzafarov AM, Kozlovsky MV, Richardson RM, et al. Liq Cryst 2001;28:1259–68. Saez IM, Goodby JW. Liq Cryst 1999;26: 1101–5.
[11] Chojnowski J, Cypryk M, Fortuniak W, Rózga-Wijas K, Scibiorek M. Polymer 2002;43:1993–2001. Chojnowski J, Cypryk M, Fortuniak W, Scibiorek M, Rozga-Wijas K. Macromolecules 2003;36:3890–7.
[12] Mauzac M, Hardouin F, Richard H, Archard MF, Sigaud G, Gasparoux H. Eur Polym J 1986;22:137–44.
[13] Itoh M, Lenz RW. J Polym Sci, Part A: Polym Chem 1991;29: 1407–12.
[14] Percec V, Heck J. J Polym Sci, Part A: Polym Chem 1991;29: 591–7.
[15] Ganicz T, Stańczyk WA. J Organomet Chem 2004;689:2606–13.
[16] Fischbach I, Pakula T, Minkin P, Fechtenkotter A, Müllen K, Spiess HW, et al. J Phys Chem B 2002;106:6408–15.
[17] Stein J, Lewis LN, Gao Y, Scott RA. J Am Chem Soc 1999;121: 3693–703.
[18] Ganicz T, Śledzińska I, Stańczyk WA, Gladkova NK. Macromolecules 2000;33:289–93. Ganicz T, Stańczyk WA. Trends Polym Sci 1997;5: 305–17.
[19] Richardson RM, Whitehouse IJ, Ponomarenko SA, Boiko NI, Shibaev VP. Mol Cryst Liq Cryst 1999;330:167–74.